589 nm laser generation by frequency doubling of a single-frequency Raman fiber amplifier in PPSLT

Lei Zhang,[1,2] Ye Yuan,[3] Yanhua Liu,[3] Jianhua Wang,[1] Jinmeng Hu,[1] Xinjie Lu,[3] Yan Feng,[1,*] and Shining Zhu[3]

[1]Shanghai Key Laboratory of Solid State Laser and Application, and Shanghai Institute of Optics and Fine Mechanics, Chinese Academy of Sciences, Qinghe Road 390, Jiading, Shanghai 201800, China

[2]Graduate University of Chinese Academy of Sciences, Beijing 100049, China

[3]Physics School of Nanjing University, Nanjing 210093, China

*Corresponding author: feng@siom.ac.cn

Received 12 December 2012; accepted 29 January 2013; posted 5 February 2013 (Doc. ID 181686); published 6 March 2013

A high-power single-frequency 1178 nm continuous-wave laser is generated in a two-stage stimulated-Brillouin-scattering-suppressed all-polarization-maintaining Raman fiber amplifier pumped by 1120 nm fiber lasers. A polarization-extinction-ratio of 30 dB is achieved due to the all-polarization-maintaining configuration and the polarization dependence gain of Raman scattering. Single-pass frequency doubling with a homemade periodically poled near-stoichiometric $LiTaO_3$ crystal (PPSLT) produces an up to 7 W narrow-linewidth laser at 589 nm. The thermally induced dephasing effect is found to be the key issue for improving second-harmonic efficiency. © 2013 Optical Society of America

OCIS codes: 140.3510, 140.3550, 190.2620.

1. Introduction

Narrow-linewidth and diffraction-limited lasers at 589 nm are required for laser-guide-star adaptive optics and laser cooling of sodium. Because of the lack of the laser gain medium which directly lases at 589 nm, frequency doubling [1] and summation [2] of laser sources at near infrared were employed to produce the 589 nm laser. Recently, fiber lasers emitting at concerning wavelengths for the generation of 589 nm lasers have received intensive attention. Yb-doped silica fiber has gain at 1178 nm, but lasing at this wavelength is difficult because of amplified spontaneous emission at shorter and higher-gain wavelengths (around 1060 nm). Various techniques, such as heating [3] of the gain fiber and a photonic bandgap fiber structure for gain engineering [4–6], have been adopted to overcome the problem. The latter has shown great potential in 1178 nm laser generation [5]. Bi-doped fiber lasers at a wavelength range of 1100–1300 nm have been demonstrated [7,8]. But the loss of Bi-doped fibers is still too high for efficient narrow-linewidth amplifier operation. 589 nm lasers can also be generated by frequency summation of a 1583 nm Er-doped fiber laser and a 938 nm Nd-doped fiber laser, but the quasi-three-level nature of the 938 nm laser has limited its output power so far [9].

The Raman fiber laser and amplifier are known for their special advantage of flexibility in wavelength, as Raman gain is available at arbitrary wavelengths across the transparency window of silica fiber (300–2300 nm) with the right pump source. The power scaling has been difficult in the narrow-linewidth Raman amplifier [10] due to the stimulated Brillouin scattering (SBS) effect. Later, high-power narrow-linewidth SBS-suppressed Raman fiber amplifiers at 1178 nm were reported [11,12]. However, the polarization state of the output was not maintained, and had to be actively controlled.

1559-128X/13/081636-05$15.00/0

To date, external-cavity resonant frequency doubling is the most efficient second-harmonic generation (SHG) technique [13,14]. An attractive alternative is the external single-pass SHG in quasi-phase-matched ferroelectric materials, which does not require active cavity length stabilization. Georgiev *et al.* reported a 3 W 589 nm laser by single-pass frequency doubling of a 23 W CW source at 1179 nm [15]. Taylor *et al.* demonstrated ~4.2 W narrowband 589 nm laser by single-pass SHG in periodically poled $KTiOPO_4$ crystal of a ~19 W CW 1178 nm laser [16]. Shirakawa *et al.* reported the generation of a 167 W laser at 1178 nm from a Yb-doped photonic bandgap fiber amplifier and then a 14.5 W laser at 589 nm by single-pass SHG [17]. However, the linewidth of the 1178 nm laser (1.3 nm) is too wide, and power scaling of the narrow-linewidth (<1 GHz) 589 nm laser is difficult.

We had previously reported a 4 W yellow light generation by single-pass frequency doubling of a Raman fiber amplifier in periodically poled near-stoichiometric $LiTaO_3$ crystal (PPSLT) [18]. In this paper, we report a detailed study with improved results. An up to 40 W single-frequency laser at 1178 nm is achieved by a two-stage Raman fiber amplifier. With a homemade PPSLT crystal, an up to 7 W laser at 589 nm with diffraction-limited beam quality is achieved by single-pass SHG with a conversion efficiency of 20%. By investigating the temporal behavior of SHG, the thermal dephasing effect in the PPSLT crystal is found to be the key issue for a further increase of the SHG efficiency.

2. Experiment Setup

The experimental configuration is shown in Fig. 1. The seed is an 1178 nm distributed feedback laser diode laser (Toptica Photonics AG, DL100) with a maximum fiber pigtailed output of 10 mW and a specified linewidth of ~1 MHz. The pump sources used for the first- and second-stage amplifiers are homemade 20 and 85 W CW linearly polarized Yb-doped single-mode fiber lasers lasing at 1120 nm [19]. At each stage, one PM 1120/1178 nm wavelength division multiplexing (WDM) is employed to couple the pump lasers into the Raman amplifier, and two WDMs are used to extract the residual pump lasers. The gain fibers used for the first and second stages are 200 m strained PM980 fiber and 52 m strained PM980 fiber, respectively. The strain distribution on the fiber to suppress the SBS effect is designed according to [20]. The spectrum of 1178 and 589 nm output is analyzed by spectrometers YOKOGAWA AQ6370B with 0.02 nm resolution and ELIAS III Echelle with 0.2 pm resolution at 589 nm, respectively. The power of the backward-propagating light from the amplifier is monitored from port A of the first WDM in the second amplifier. A PM isolator is inserted between the two stages to isolate the backward-propagating light. The output delivery fiber is 8° angle cleaved to avoid reflection from the end face. An aspheric lens F1 with a focus length of 11 mm is used to collimate the output laser, and a focusing lens F2 with a focus length of 150 mm is adopted to focus the light to the nonlinear crystal. A half-wave plate is adopted to ensure that the output polarization is parallel to the poling direction of the crystal. The frequency-doubling crystal is a homemade 39 mm long PPSLT fabricated by an improved electrical poling technique, with a period of $\Lambda = 10.4$ μm according to the quasi-phase-matching condition. The crystal is housed in a homemade oven with a temperature stability of ±0.1°C. The crystal end faces have high transmission of $T > 95\%$ at 589 nm and low reflectivity of $R < 0.5\%$ at 1178 nm. The generated yellow light and the input fundamental light are separated by a dichroic mirror ($R > 99.5\%$ at 1178 nm and $T > 94\%$ at 589 nm).

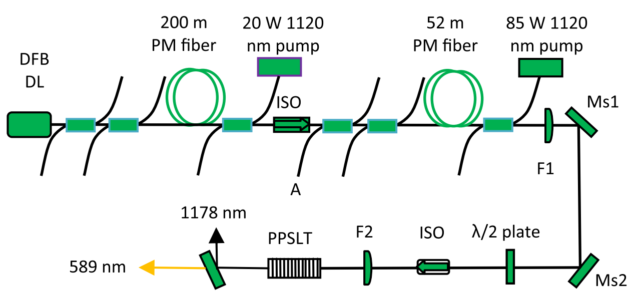

Fig. 1. (Color online) Schematic diagram of the experimental configuration.

3. Experimental Results and Discussions

After the first-stage amplifier, the 1178 nm laser is amplified to 0.8 W. Figure 2 shows the output power and backward-propagating light from the second Raman amplifier as a function of pump power. At the time of conducting the single-pass SHG experiments, the maximum output power was scaled to 39.3 W, corresponding to 46.2% optical conversion efficiency. The maximum power of the backward-propagated light is 0.63 W, indicating that SBS is effectively suppressed by applying variable strain to the gain fiber. Please note that the backward light contains not only backward light but also Raman-amplified Rayleigh scattering and the remaining 1120 nm pump light. An optical spectral

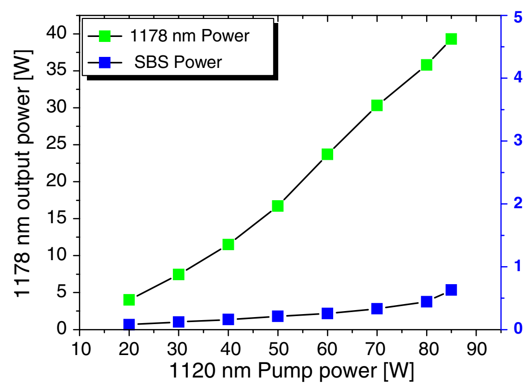

Fig. 2. (Color online) Raman amplifier output power and backward-propagating light as a function of pump power.

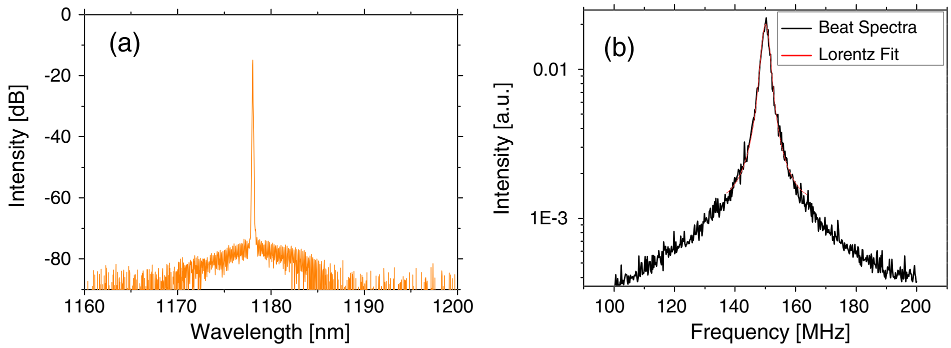

Fig. 3. (Color online) (a) Output spectrum of the laser. (b) Self-heterodyne beat spectra of the 1178 nm laser (black) and the Lorentzian fit of the beat spectrum (red).

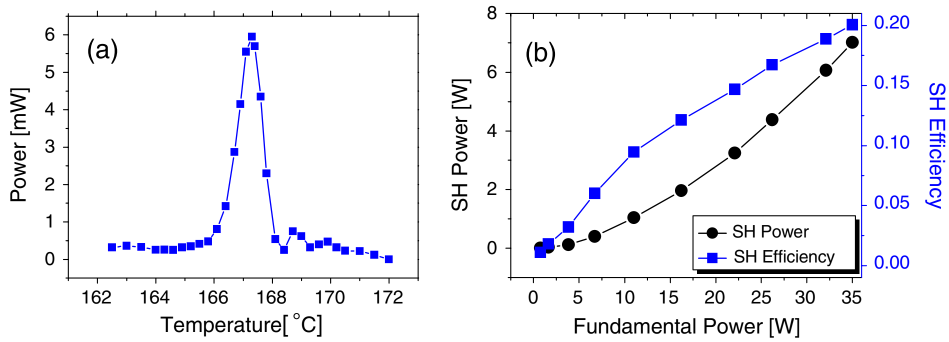

Fig. 4. (Color online) (a) Temperature tuning curves under approximately 1 W fundamental power through the crystals. (b) SH power (circle) and conversion efficiency (square) as a function of the fundamental power at a temperature of 168.8°C.

analyzer (YOKOGAWA AQ6370) is used to check the spectral purity of the laser output. The signal-to-noise ratio is found to be 60 dB, as shown in Fig. 3(a). The linewidth is measured by a self-heterodyne method. The output of the Raman fiber laser was divided into two paths. One path was sent through a 1000 m PM980 delay line. The other path was connected with a fiber pigtailed acousto-optic modulator with a carrier frequency shift of 150 MHz. The light was recombined and detected with a 2 GHz photodiode and analyzed with a high-resolution rf-spectrum analyzer (Agilent E4405B). And a Lorentzian fit of the output radio-frequency spectrum indicates the laser has a linewidth of 1 MHz at the maximum output power, which is shown in Fig. 3(b). Linearly polarized output with a polarization-extinction ratio of 30 dB is achieved due to the all-polarization-maintaining configuration and the polarization-dependent gain of Raman scattering.

Temperature tuning curves are measured with 1 W of fundamental light directed through the crystals. As shown in Fig. 4(a), the temperature tolerance of the PPSLT crystal is 1.0°C and the optimum phase-matching temperature is 167.3°C. Figure 4(b) shows second-harmonic power and SHG efficiency as a function of the fundamental laser power at a temperature of 168.8°C. The maximum SHG output power is 7 W, corresponding to a conversion efficiency of 20%. However, an obvious rolloff in the conversion efficiency curve is observed after the input fundamental power exceeds 10 W, which can be attributed to thermal dephasing in the crystal [21,22], which will be discussed later. Figure 5 depicts the fine spectrum of SHG light with a high-precision optical spectrum (ELIAS III Echelle). The FWHM linewidth is measured to be 0.198 pm limited by the resolution of the spectrum. The actual linewidth should be ~2 MHz, since the fundamental laser has a linewidth of 1 MHz. An M^2 factor of 1.28 at the highest output power is measured by a laser beam analyzer (Primes LQM-HP), which shows slight beam quality degrading in the PPSLT crystal.

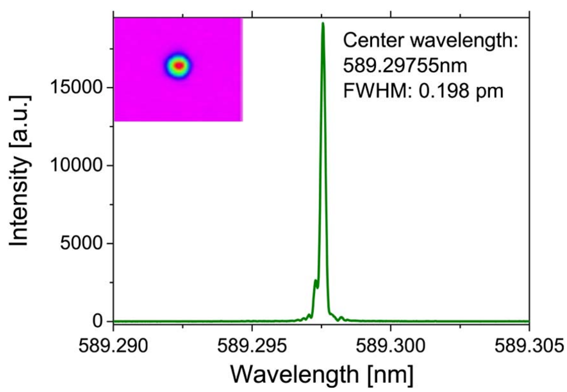

Fig. 5. (Color online) Spectrum of the 589 nm laser at the highest output power (7 W). Inset: far-field beam profile of the 589 nm laser.

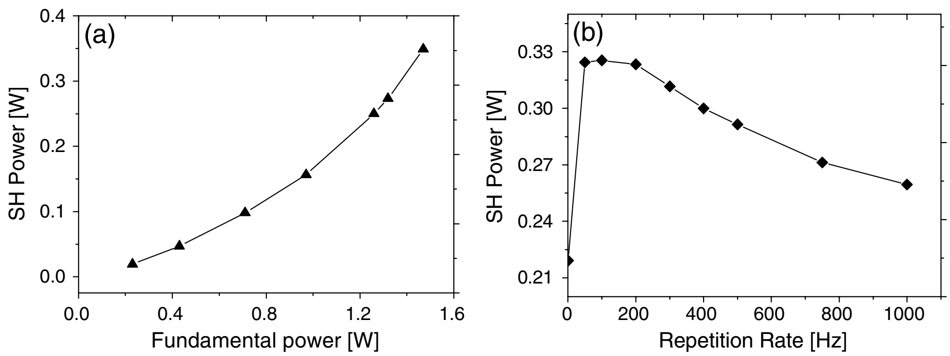

Fig. 6. SH power as a function of (a) fundamental power modulated at 500 Hz with a 5.0% duty cycle and (b) different repetition rate with a 5.0% duty cycle.

A far-field beam profile of the 589 nm laser is shown in the inset of Fig. 5.

To investigate the thermal effect in the PPSLT crystal on the SHG process, we study the SHG in quasi-CW modes, in which cases thermal loading is lower. The quasi-continuous wave 1178 nm laser is obtained by modulating the 1120 nm pump laser of the second amplifier. The resulting pulses have a 0.8 W CW floor. First we modulate the fundamental laser with a repetition rate of 500 Hz and a pulse duration of 100 μs. Figure 6(a) shows the resulting second-harmonic power and conversion efficiency versus the average fundamental power, where the power for the CW floor of the fundamental laser has been deducted. Each data point is taken with optimized oven temperature. The efficiency rolloff is largely overcome. The conversion efficiency increases by 5.6% at 30 W peak power (23.6%) compared to the corresponding CW case (18.1%). Figure 6(b) illustrates the SHG efficiency as a function of the pulse repetition at the same average fundamental power (1.32 W) and duty cycle (5%). The conversion efficiency peaks at around 100 Hz. The SHG power and efficiency decrease almost linearly when the pulse repetition is greater than 200 Hz. When the repetition rate is lower than 100 Hz, the conversion efficiency decreases as well and approaches the CW case. The observation proves that the thermal-induced dephasing indeed contributes significantly to the relatively low SH efficiency. It also indicates that the thermal equilibrium process in the PPSLT crystal has a time constant of around 10 ms. At a higher repetition rate, the heat deposition from successive pulses is cumulated. At a lower repetition rate, the pulses are long enough for heat equilibrium to be achieved within a single pulse.

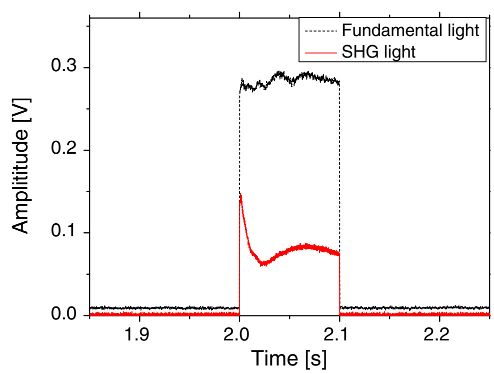

Fig. 7. (Color online) Fundamental light (dashed) and SHG light (solid) time-domain signals at repetition rate 0.5 Hz.

To observe the time evolution of the SHG due to the thermal effects, we modulate the 1178 nm amplifier at a very low repetition rate of 0.5 Hz, 30 W peak power, and 5% duty cycle to avoid any heat accumulation from successive pulses. As shown in Fig. 7, the power of second-harmonic light decreases quickly at the first 10 ms. After that, the power fluctuates slowly during the rest of the pulse. This suggests a very long time is needed to achieve the final temperature equilibrium, and the instantaneous SHG efficiency is much higher than stabilized efficiency. Therefore, there is much room for improving the conversion efficiency if the thermal dephasing effect is reduced.

4. Conclusion

In conclusion, we achieved a high-power linearly polarized 1178 nm continuous-wave laser by two-stage PM Raman fiber amplifiers. With a homemade PPSLT crystal and temperature oven, 7.0 W 589 nm yellow light is obtained in a simple single-pass SHG device. We experimentally verify that the thermal effect on the crystal influences the SHG efficiency greatly. Future work will concentrate on designing a better oven to reduce the temperature inhomogeneity in the crystal at high-power pumping. A shorter crystal might be also helpful in alleviating the thermal dephasing. We believe the SHG conversion efficiency can be improved after all these optimizations.

The work is supported by the Hundred Talent Program of the Chinese Academy of Sciences.

References

1. Y. Feng, S. Huang, A. Shirakawa, and K. Ueda, "589 nm light source based on Raman fiber laser," Jpn. J. Appl. Phys. **43**, L722–L724 (2004).
2. J. C. Bienfang, C. A. Denman, B. W. Grime, P. D. Hillman, G. T. Moore, and J. M. Telle, "20 W of continuous-wave sodium D2 resonance radiation from sum-frequency generation with injection-locked lasers," Opt. Lett. **28**, 2219–2221 (2003).
3. M. P. Kalita, S.-u. Alam, C. Codemard, S. Yoo, A. J. Boyland, M. Ibsen, and J. K. Sahu, "Multi-watts narrow-linewidth all

fiber Yb-doped laser operating at 1179 nm," Opt. Express **18**, 5920–5925 (2010).
4. A. Shirakawa, H. Maruyama, K. Ueda, C. B. Olausson, J. K. Lyngsø, and J. Broeng, "High-power Yb-doped photonic bandgap fiber amplifier at 1150–1200 nm," Opt. Express **17**, 447–454 (2009).
5. C. B. Olausson, A. Shirakawa, M. Chen, J. K. Lyngsø, J. Broeng, K. P. Hansen, A. Bjarklev, and K. Ueda, "167 W, power scalable ytterbium-doped photonic bandgap fiber amplifier at 1178 nm," Opt. Express **18**, 16345–16352 (2010).
6. M. Chen, A. Shirakawa, X. Fan, K.-i. Ueda, C. B. Olausson, J. K. Lyngsø, and J. Broeng, "Single-frequency ytterbium doped photonic bandgap fiber amplifier at 1178 nm," Opt. Express **20**, 21044–21052 (2012).
7. A. B. Rulkov, A. A. Ferin, S. V. Popov, J. R. Taylor, I. Razdobreev, L. Bigot, and G. Bouwmans, "Narrow-line, 1178 nm CW bismuth-doped fiber laser with 6.4 W output for direct frequency doubling," Opt. Express **15**, 5473–5476 (2007).
8. V. V. Dvoyrin, V. M. Mashinsky, and E. M. Dianov, "Efficient bismuth-doped fiber lasers," IEEE J. Quantum Electron. **44**, 834–840 (2008).
9. J. W. Dawson, A. D. Drobshoff, R. J. Beach, M. J. Messerly, S. A. Payne, A. Brown, D. M. Pennington, D. J. Bamford, S. J. Sharpe, and D. J. Cook, "Multi-watt 589 nm fiber laser source," Proc. SPIE **6102**, 61021F (2006).
10. Y. Feng, L. Taylor, and D. Bonaccini Calia, "Multiwatts narrow linewidth fiber Raman amplifiers," Opt. Express **16**, 10927–10932 (2008).
11. Y. Feng, L. R. Taylor, and D. B. Calia, "25 W Raman-fiber-amplifier-based 589 nm laser for laser guide star," Opt. Express **17**, 19021–19026 (2009).
12. L. R. Taylor, Y. Feng, and D. B. Calia, "50 W CW visible laser source at 589 nm obtained via frequency doubling of three coherently combined narrow-band Raman fibre amplifiers," Opt. Express **18**, 8540–8555 (2010).
13. Z. Y. Ou, S. F. Pereira, E. S. Polzik, and H. J. Kimble, "85% efficiency for cw frequency doubling from 1.08 to 0.54 μm," Opt. Lett. **17**, 640–642 (1992).
14. T. Sudmeyer, Y. Imai, H. Masuda, N. Eguchi, M. Saito, and S. Kubota, "Efficient 2nd and 4th harmonic generation of a single-frequency, continuous-wave fiber amplifier," Opt. Express **16**, 1546–1551 (2008).
15. D. Georgiev, V. P. Gapontsev, A. G. Dronov, M. Y. Vyatkin, A. B. Rulkov, S. V. Popov, and J. R. Taylor, "Watts-level frequency doubling of a narrow line linearly polarized Raman fiber laser to 589 nm," Opt. Express **13**, 6772–6776 (2005).
16. L. Taylor, Y. Feng, D. B. Calia, and W. Hackenberg, "Multi-watt 589 nm Na D[sub 2]-line generation via frequency doubling of a Raman fiber amplifier: a source for LGS-assisted AO," Proc. SPIE **6272**, 627249 (2006).
17. A. Shirakawa, C. B. Olausson, M. Chen, K.-i. Ueda, J. K. Lyngsø, and J. Broeng, "Power-scalable photonic bandgap fiber sources with 167 W, 1178 nm and 14.5 W, 589 nm radiations," in *Advanced Solid-State Photonics*, OSA Technical Digest (CD) (Optical Society of America, 2010), paper APDP6.
18. Y. Yuan, L. Zhang, Y. Liu, X. Lü, G. Zhao, Y. Feng, and S. Zhu, "Sodium guide star laser generation by single-pass frequency doubling in a periodically poled near-stoichiometric $LiTaO_3$ crystal," Sci. China Technol. Sci. **56**, 125–128 (2013).
19. J. Wang, L. Zhang, J. Hu, L. Si, J. Chen, X. Gu, and Y. Feng, "Efficient linearly polarized ytterbium-doped fiber laser at 1120 nm," Appl. Opt. **51**, 3801–3803 (2012).
20. L. Zhang, J. Hu, J. Wang, and Y. Feng, "Stimulated-Brillouin-scattering-suppressed high-power single-frequency polarization-maintaining Raman fiber amplifier with longitudinally varied strain for laser guide star," Opt. Lett. **37**, 4796–4798 (2012).
21. O. A. Louchev, N. E. Yu, S. Kurimura, and K. Kitamura, "Nanosecond pulsed laser energy and thermal field evolution during second harmonic generation in periodically poled $LiNbO_3$ crystals," J. Appl. Phys. **98**, 113103 (2005).
22. S. V. Tovstonog, S. Kurimura, I. Suzuki, K. Takeno, S. Moriwaki, N. Ohmae, N. Mio, and T. Katagai, "Thermal effects in high-power CW second harmonic generation in Mg-doped stoichiometric lithium tantalate," Opt. Express **16**, 11294–11299 (2008).